Structure of the SHV-1 β-Lactamase†

Alexandre P. Kuzin,‡ Michiyoshi Nukaga,‡,§ Yasuko Nukaga,‡ Andrea M. Hujer,|| Robert A. Bonomo,|| and James R. Knox*,‡

Department of Molecular and Cell Biology, The University of Connecticut, Storrs, Connecticut 06269-3125, and Research Service, Department of Veterans Affairs Medical Center, Cleveland, Ohio 44106

Received January 20, 1999; Revised Manuscript Received March 3, 1999

ABSTRACT: The X-ray crystallographic structure of the SHV-1 β-lactamase has been established. The enzyme crystallizes from poly(ethylene glycol) at pH 7 in space group $P2_12_12_1$ with cell dimensions $a = 49.6$ Å, $b = 55.6$ Å, and $c = 87.0$ Å. The structure was solved by the molecular replacement method, and the model has been refined to an *R*-factor of 0.18 for all data in the range 8.0−1.98 Å resolution. Deviations of model bonds and angles from ideal values are 0.018 Å and 1.8°, respectively. Overlay of all 263 α-carbon atoms in the SHV-1 and TEM-1 β-lactamases results in an rms deviation of 1.4 Å. Largest deviations occur in the H10 helix (residues 218−224) and in the loops between strands in the β-sheet. All atoms in residues 70, 73, 130, 132, 166, and 234 in the catalytic site of SHV-1 deviate only 0.23 Å (rms) from atoms in TEM-1. However, the width of the substrate binding cavity in SHV-1, as measured from the 104−105 and 130−132 loops on one side to the 235−238 β-strand on the other side, is 0.7−1.2 Å wider than in TEM-1. A structural analysis of the highly different affinity of SHV-1 and TEM-1 for the β-lactamase inhibitory protein BLIP focuses on interactions involving Asp/Glu104.

β-Lactamase enzymes (EC 3.5.2.6) hydrolyze β-lactam antibiotics and are the principal agent of bacterial resistance to penicillins and cephalosporins (*1*−*3*). They have been

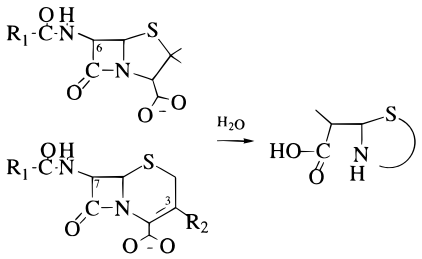

grouped into four classes (A to D) on the basis of amino acid sequences and motifs (*4*) and into subgroupings as well on the basis of substrate/inhibitor profiles (*5*). Class A β-lactamases, originally designated penicillinases, include many of the plasmid-mediated enzymes from Gram-negative bacteria and chromosomal enzymes from Gram-positive bacteria. Class C β-lactamases include the chromosomal cephalosporinases of Gram-negative bacteria. Class D β-lactamases are unique penicillinases with the ability to hydrolyze oxacillin, a semisynthetic penicillin stable to many β-lactamases. Although class A, C, and D β-lactamases are serine-reactive hydrolases, class B enzymes are zinc hydrolases with a broader substrate profile than the other classes.

Among the four β-lactamase classes, the class A enzymes are the most frequently encountered in clinical isolates because of plasmid selection and transfer in response to the introduction of new β-lactams. "Extended-spectrum" class A β-lactamases are variants of a parental type and have one to five amino acid substitutions for better hydrolysis of second and third generation cephalosporins (*6*). As well, inhibitor-resistant class A β-lactamases, having low affinity for heavily used inhibitors such as clavulanic acid, sulbactam, or tazobactam, have been isolated (*7*, *8*).

This evolution of plasmid-encoded extended-spectrum and inhibitor-resistant variants is progressing rapidly in the clinically prevalent TEM- and SHV-type β-lactamases. The parental forms, TEM-1 and SHV-1, were first reported in 1963 and 1974, respectively, and have spread among bacterial species so that now there are more than 60 variants of the TEM-type gene and 12 variants of SHV (*9*). Crystallographic study of the plasmid-encoded TEM-type enzyme was initiated in the early 1970s (*10*) and was completed at high resolution in the 1990s (*11*−*13*). Here we report the structure of SHV-1, the β-lactamase predominating in ampicillin-resistant *Klebsiella pneumoniae* and the prototype of the growing family of SHV variants. The availability of this parental SHV structure will put on firmer ground the structure-based modeling of SHV variants.

MATERIALS AND METHODS

Gene Cloning and Enzyme Purification. The SHV-1 β-lactamase gene (*bla*) was directionally subcloned into the phagemid vector pBCSK (Stratagene, La Jolla, CA) from a clinical strain of *K. pneumoniae* 15571 (A. Hujer, L. Rice, V. Anderson, and R. Bonomo, unpublished results). The DNA sequence of the bla_{SHV-1} gene in this report has been deposited into GenBank (Accession No. AF124984). *Escherichia coli* DH10B [F⁻*mcr*A Δ(*mrr-hsd*RMS-*mcr*BC) φ80d*lac*ZΔ*M*15 Δ*lac*X74 *deo*R *rec*A1 *end*A1 *ara*D139 Δ(*ara*, *leu*)7697*gal*U *gal*K λ⁻*rps*L *nup*G] was the host strain

† This work was supported by grants from the Department of Veterans Affairs to R.A.B. and J.R.K. and from the National Institute of Aging (NIH/NIA AG-00634) to R.A.B.

* Corresponding author: phone 860-486-3133; fax 860-486-4745; e-mail knox@uconnvm.uconn.edu.

‡ The University of Connecticut.

§ Permanent address: Faculty of Pharmaceutical Sciences, Chiba University, Chiba 263, Japan.

|| Department of Veterans Affairs Medical Center.

10.1021/bi990136d CCC: $18.00
Published on Web 04/20/1999

used to harvest the SHV-1 enzyme (Gibco BRL, Grand Island, NY). A 5 mL overnight culture from a single colony of *E. coli* with bla_{SHV-1} was used to inoculate 1.5 L of Luria−Bertani broth containing 100 μg/mL ampicillin and 20 μg/mL chloramphenicol (Sigma, St. Louis, MO). Cells were grown for 16−20 h to stationary phase. Cell pellets were obtained from overnight cultures and were stored at −20 °C until purification.

The enzyme was liberated by stringent periplasmic fractionation using lysozyme and EDTA (*14*, *15*). Crude lysates were clarified by filtration (0.22 μm) and concentrated with a Diaflo ultrafiltration membrane (Amicon, Inc., Beverly, MA) having a 10 kDa molecular mass cutoff. The β-lactamase was purified using preparative isoelectric focusing in a Multiphor II apparatus (Pharmacia, Piscataway, NJ) in an Ultradex gel bed containing 2% ampholines through a pH gradient of 6−8. The gel was run overnight at 4 °C with limiting conditions at 2000 V, 50 mA, and constant power (8 W). β-Lactamase activity was identified by applying finely cut strips of filter paper to the top of the gel and observing the yellow-to-pink color change after application of a 100 μM solution of nitrocefin (Becton-Dickinson, Cockeysville, MD) to the paper. Areas containing β-lactamase activity were cut from the gel, placed in PEGG columns (Pharmacia), and eluted with 20 mM diethanolamine buffer, pH 8.3. To remove ampholines, the eluate (approximately 15 mL) was dialyzed 18 h at 4 °C in 1.5 L of diethanolamine buffer. Samples were concentrated by ultrafiltration. Purity of fractions was assessed using Coomassie Blue stained 12% SDS−PAGE gels. Protein concentrations were determined with the Bio-Rad Protein Assay (Bio-Rad, Hercules, CA).

Crystallization. Crystals having cubic morphology and measuring up to 0.3 mm were grown at room temperature by the vapor diffusion method. The 25 μL sitting protein drop [2 mg/mL, 0.56 mM Cymal-6 detergent (1 cmc, Anatrace, Maume, OH), 15% poly(ethylene glycol) (M_r = 6000, Hampton Research, Lagnua Niguel, CA), 50 mM HEPES buffer, pH 7.0] was placed over a 0.75 mL reservoir solution containing 30% poly(ethylene glycol) and 100 mM HEPES buffer. The enzyme crystallized in 1 week in the orthorhombic space group $P2_12_12_1$ with cell dimensions a = 49.6 Å, b = 55.6 Å, and c = 87.0 Å and one molecule in the asymmetric unit (2.08 Å^3/Da; 41% solvent volume). Of many additives tested in order to optimize the crystallization with PEG, two components of a 24-detergent screen kit (Hampton Research), Cymal-5 and -6, were found necessary for improving crystal size, morphology, and, especially, mechanical robustness. Crystals from Cymal-6 were used for data collection.

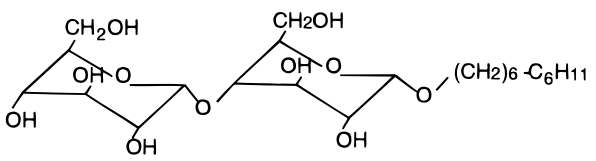

X-ray Data Collection. Data were collected at 20 °C from a capillary-mounted crystal on a Bruker Histar multiwire area detector on a Rigaku RU-200 rotating anode generator operating at 40 kV and 60 mA with a 3 mm filament (Cu Kα radiation) and double-mirror Franks focusing. At a detector distance of 10 cm, 1024 × 1024 pixel frames were counted for 120 s through an ω step of 0.2°. Data were reduced and scaled with XGEN (Molecular Simulations, Inc.) to an R_{sym} = 0.065 for 15 082 unique reflections from 49 725 observations for an overall completeness of 85%. Data statistics are summarized in Table 1.

Table 1: X-ray Data Collection and Reduction

temp (°C)	20	highest shell, d (Å)	2.09−1.96
d_{min} [for 3$\sigma(I)$] (Å)	1.97 (1.99)	observations	2259
observations	49725	unique reflections	1156
unique reflections	15082	completeness	0.40
completeness	0.85	av $I/\sigma(I)$	3.2
av $I/\sigma(I)$	15.5	$R_{sym}(I)$[a]	0.194
$R_{sym}(I)$[a]	0.065		

[a] $R_{sym} = \sum|I_{av} - I_i|/\sum I_i$, where I_{av} is the average of all individual observations, I_i. The space group is $P2_12_12_1$.

RESULTS

Structure Determination. The crystal structure was solved by molecular replacement using as a search model the structure of the homologous TEM-1 β-lactamase [(*13*), Protein Data Bank, 1XPB], which has 68% sequence identity with the 28 874 Da SHV-1 enzyme (Figure 1). With the program AMoRe (*16*) and an integration radius of 24 Å for all data in the resolution range from 8 to 4 Å, two solutions were found having correlation coefficients 29% and 15%. When both solutions were used in a translation search, only the first produced a significantly better correlation coefficient and R-factor (47% and 44%, respectively). Rigid body refinement improved these parameters to 50% and 42%.

Structure Refinement. The initial electron density map was generally complete along the entire polypeptide chain and showed side chain densities expected for the SHV-1 enzyme. Two cycles of manual fitting of the SHV-1 sequence (GenBank AF124984; A. Hujer, L. Rice, V. Anderson, and R. Bonomo, unpublished results) using the program CHAIN (*17*) were done to optimize backbone and side chain positions, especially near helix H10 from position 218 to 228. Simulated annealing refinement was initiated at 1500 K with X-PLOR (*18*). Maps using all data from 21 to 1.98 Å showed significant electron density later attributable to one molecule of Cymal-6 detergent. To chose protein side chain rotatmers and water positions, hydrogen-bonding patterns and B-factors were examined carefully. Final annealing cycles were started at 500 K and used weights to restrain water positions. For a model which included all 265 amino acid residues, one Cymal-6 molecule, and 81 water molecules (B-factors < 50 Å^2), the resulting crystallographic R-factor is 0.182 for all nonzero data in the range 8.0−1.98 Å. The R_{free} value is 0.254 (*19*). Deviations of the protein model from ideality are 0.018 Å and 1.8° for covalent bonds and angles, respectively. From a plot of R-factor vs resolution the coordinate error is estimated to be 0.21 Å. Conformation analysis shows that non-glycine residues with less-favored backbone conformations include catalytic site residues Met69, Tyr105, and Ser130, as observed in other class A β-lactamases (*12*, *13*, *20*−*22*). Others with positive ϕ and ψ angles are 61, 172, 179, 241, 254, 255, and 267. A β-lactamase residue expected to have a high-energy conformation, Leu220, is instead found relaxed, possibly because of the H10 movement (see below). Final refinement results are given in Table 2. The electron density map near the

```
                30          40          50          60          70          80          90          100
TEM-1        HPETL VKVKDAEDQL GARVGYIELD LNSGKILESF RPEERFPMMS TFKVLLCGAV LSRVDAGQEQ LGRRIHYSQN
             * **  *** ** *   **   *  *   *  ** ***  **           *        *           * *   * *
SHV-1        SPQPL EQIKLSESQL SGRVGMIEMD LASGRTLTAW RADERFPMMS TFKVVLCGAV LARVDAGDEQ LERKIHYRQQ

               110         120         130         140         150         160         170         180
TEM-1    DLVEYSPVTE KHLTDGMTVR ELCSAAITMS DNTAANLLLT TIGGPKELTA FLHNMGDHVT RLDRWEPELN EAIPNDERDT
           *    *     *     *    *           *      *   *   **     ***  *          *      * * *
SHV-1    DLVDYSPVSE KHLADGMTVG ELCAAAITMS DNSAANLLLA TVGGPAGLTA FLRQIGDNVT RLDRWETELN EALPGDARDT

               190         200         210         220         230         240         250         260
TEM-1    TMPAAMATTL RKLLTGELLT LASRQQLIDW MEADKVAGPL LRSALPAGWF IADKSGAG-E RGSRGIIAAL GP-DGKPSRI
          *  *  *       *** * ** **  **   ** *      *  *             *        *   * *     ** **
SHV-1    TTPASMAATL RKLLTSQRLS ARSQRQLLQW MVDDRVAGPL IRSVLPAGWF IADKTGAG-E RGARGIVALL GP-NNKAERI

               270         280         290
TEM-1    VVIYTTGSQA TMDERNRQIA EIGASLIKHW --
             *****  * *   *    *   *  *   **
SHV-1    VVIYLRDTPA SMAERNQQIA GIGAALIEHW QR
```

FIGURE 1: Alignment of sequences for the mature forms of SHV-1 and TEM-1 β-lactamases. The consensus numbering for class A β-lactamases (*41*) results in deletions in both enzymes at positions 239 and 253. Differing positions are marked.

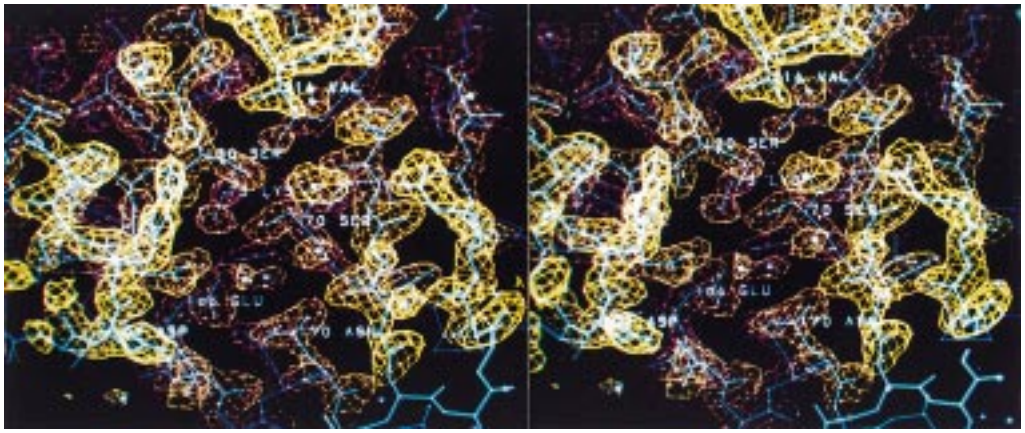

FIGURE 2: Stereoview of the $2F_o - F_c$ electron density around the catalytic site from FRODO (*42*). The contour level is 1.5σ.

Table 2: Crystallographic Refinement

resolution range (Å)	8.0−1.98
no. of reflections used [$F > 0\sigma(F)$]	13653
R-factor	0.182
R_{free} factor[a]	0.254
rms deviations from ideality	
bond lengths (Å)	0.018
bond angles (deg)	1.8
planarity (deg)	1.5
mean *B*-factors (Å^2)	
protein	14.1
detergent	21.0
water	26.8
all atoms	14.7

[a] Calculated from 6.6% of the reflections omitted from refinement.

catalytic site is shown in Figure 2. Atomic coordinates have been deposited in the Protein Data Bank (Entry 1SHV) at Rutgers University.

Detergent Binding. The electron density map showed clear density for a single molecule of the detergent included in the crystallization media (Figure 3a). The hydrocarbon tail of Cymal-6 is surrounded by hydrophobic residues from the β-sheet and two α-helices, H10 (218−224) and H11 (272−289), on the face of the β-sheet. Some residues contacting the detergent tail are isoleucines 221, 231, 246, 263, and 287, valines 224 and 261, leucines 225 and 250, alanines 280 and 248, and glycine 283. The solvent-exposed disaccharide group is hydrogen bonded to surface residues 93−96 in the all-helix domain of a neighboring molecule (Figure 3b,c). To our knowledge, this is the first observation of a complete, undisordered molecule of detergent directly facilitating intermolecular aggregation and crystallization.

To establish whether the bound detergent molecule, about 17 Å from the reactive Ser70, could alter the catalytic competence of the enzyme, activity measurements were performed with Cymal-6 in the crystal and in solution. Nitrocefin, a chromophoric cephalosporin, was added to the crystal's holding solution at 3−5 mM. After 15−20 min, the crystal turned red, indicating enzymic activity in the crystal. Measurements of activity in a solution of SHV-1 containing 0.6 mM Cymal-6 showed approximately 20% and 25% reductions in reaction velocity for nitrocefin and penicillin-G (Fluka, Ronkonkoma, NY), respectively. Initial rates were determined during the first 5−10% of the reaction in 20 mM sodium phosphate buffer at pH 7.4 with 100 μM substrate and 11.5 nM enzyme. The corresponding molar extinction coefficients used with a Hewlett-Packard 8452 spectrophotometer were $\Delta\epsilon = 17\,400$ M^{-1} cm^{-1} at 482 nm and $\Delta\epsilon = 529$ M^{-1} cm^{-1} at 240 nm, respectively (*23*).

DISCUSSION

SHV-1 and Its Comparison with TEM-1. The SHV-1 β-lactamase has two domains, one is entirely α-helical and the second consists of a five-stranded antiparallel β-sheet

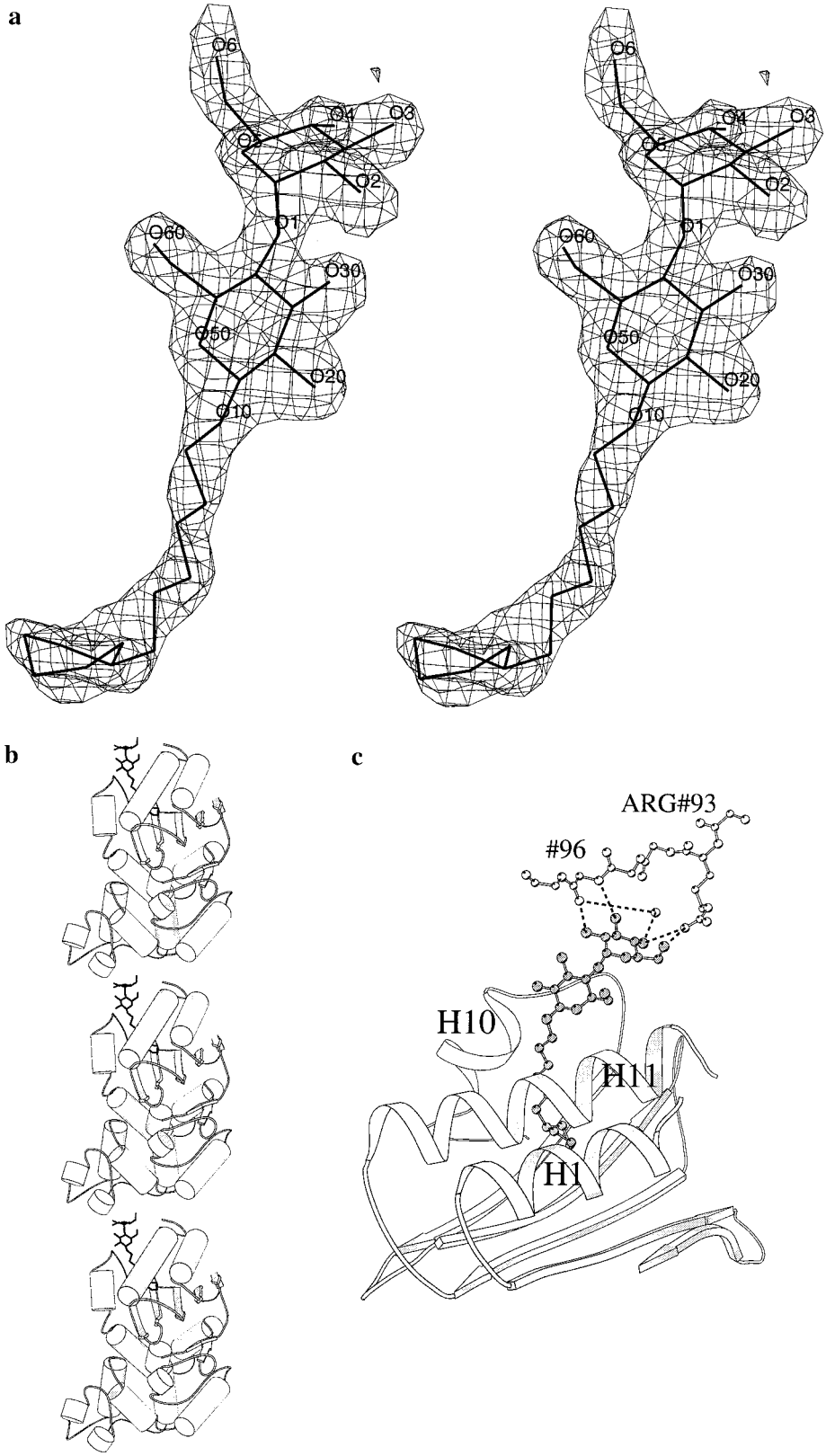

FIGURE 3: (a) Stereoview of the $2F_o - F_c$ electron density of Cymal-6 at a contour level of 1.35σ from CHAIN (*17*). (b) MOLSCRIPT (*43*) view of the crystal packing of β-lactamase. The detergent links SHV-1 molecules along the *a* direction of the lattice. (c) MOLSCRIPT diagram showing intermolecular hydrogen bonding via the maltose moiety of Cymal-6.

surrounded on both sides by α-helices (Figure 4). The general fold of the enzyme resembles that seen in other class A β-lactamase crystal structures, whether plasmid-encoded or chromosomal (see ref *24*). The closest homologue of the plasmid-encoded SHV-1 enzyme is the TEM-1 enzyme, which has a 68% identical sequence (Figure 1) and a similar substrate specificity profile. However, in response to the introduction of novel β-lactams and mechanism-based inhibitors, the genes of the two parental β-lactamases are rapidly evolving by somewhat separate pathways, and further,

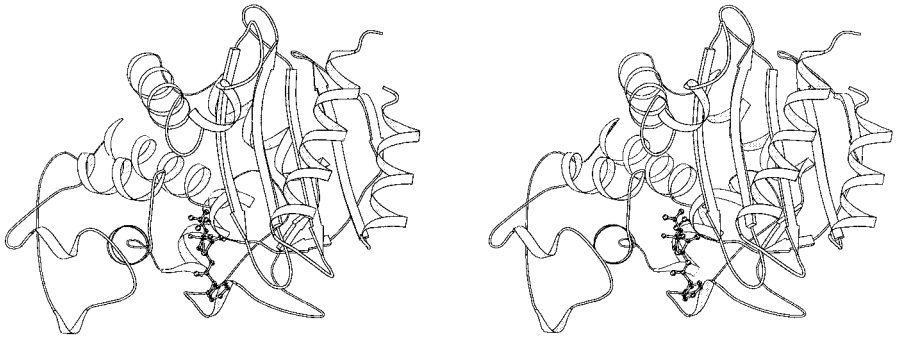

FIGURE 4: Stereoview of the SHV-1 β-lactamase drawn by MOLSCRIPT (*43*). Ampicillin has been docked to show the position of the β-lactam binding site near Ser70.

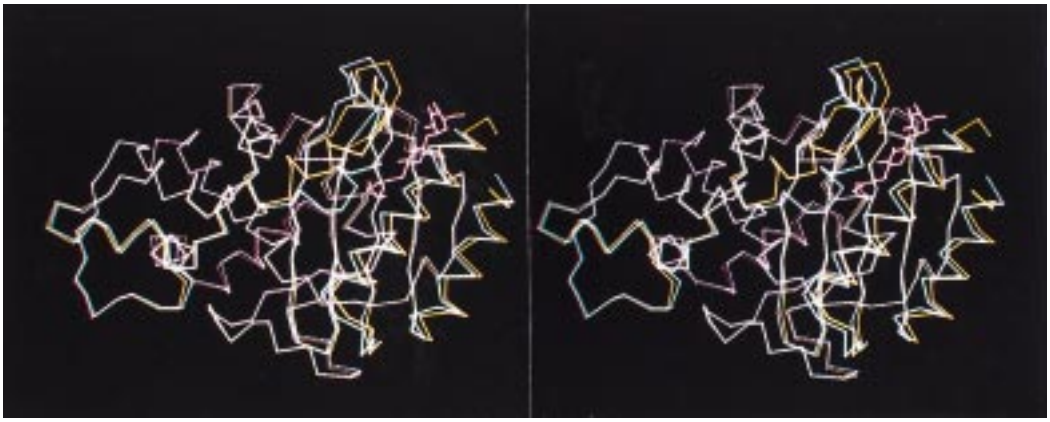

FIGURE 5: Overlay of α-carbon atoms in SHV-1 (yellow) and TEM-1 (1XPB, dashed blue) from FRODO (*42*). The rms deviation for all 263 carbon atoms is 1.39 Å. The detergent molecule bound to SHV-1 is shown in pink.

the two β-lactamases exhibit affinities for the β-lactamase inhibitory protein (BLIP) differing by 3−4 orders of magnitude (*25*). A comparison of the SHV-1 with TEM-1 prototypes may reveal structural factors contributing to these puzzling observations.

Most of the 12−15 nonconservative sequence differences in the two enzymes occur at solvent-exposed positions 92, 98, 100, 120, 146, 147, 198, 201, 202, 212, 213, 255, 273, and 281. Changes at neighboring positions 266 (Thr to Arg in SHV-1) and 267 (Gly to Asp) result in longer side chains which may stabilize the Ω loop (160−181) via several solvation bridges. Other significant changes will be discussed below.

α-Carbon atoms of the SHV-1 and TEM-1 (1XPB) enzymes overlay within an rms deviation of 1.4 Å (Figure 5). For comparison, the overlay of TEM-1 with the β-lactamases of *Bacillus licheniformis* 749/C (4BLM) and *Staphylococcus aureus* PC1 (3BLM) gives rms deviations of 2.0 and 2.4 Å, respectively. For the SHV/TEM pair the deviations greater than the rms value occur at the N-terminus, at the 38−39 and 252−256 loops near β-strands, and at 218−230 in the H10 α-helix. It is possible that some or all of the H10 displacement, from 2 to 8 Å relative to TEM-1, is due to the nearby binding of the detergent molecule. Correlated with the displacement of H10 is a backbone rotation at Val 216 above the substrate binding site, and this might be the cause of the reduction in enzymatic activity measured in the presence of Cymal-6 detergent (see Results).

Catalytic Site. The six catalytically important residues (Ser70, Lys73, Ser130, Glu166, Asn170, and Lys234) in SHV-1 have individual solvent accessibilities comparable to those in other class A enzymes. Quintessential are the observed zero accessibility for Lys73 and Lys234 and the minimal but necessary accessibility for Glu166, as discussed previously (*21*). Selected distances in the catalytic site (Figure 6) are given in Table 3 and, except for a long distance between Lys73 and Asn132, are unexceptional when compared with averaged distances from other class A structures (*26*). The six residues listed above superpose with those in TEM-1 very closely with an rms deviation of 0.23 Å. However, larger differences between the two enzymes are seen at the mouth of the binding cavity. Distances from backbone atoms on the 104−105 loop or 130−132 loop across to the 235−238 β-strand are significantly greater in SHV-1 by 0.7−1.2 Å and may explain the longer Lys73 to Asn132 distance in SHV-1.

On the left side of the mouth the presence of Asp104 in SHV-1 for Glu104 in TEM-1 makes the mouth yet larger in SHV-1 and may be a determinant of the very slight differences in substrate profiles of SHV-1 and TEM-1. While in some β-lactamases the 104 side chain is hydrogen bonded to Asn132, in SHV-1 Asp104 is solvated with its backbone CO group hydrogen bonding to Asn132. Modeling has indicated that the residue at 104 may influence the positioning of the important 130−132 loop (*27*) or may simply provide favorable bonding with certain substrates (*28*). It is interesting that Glu104 in TEM-1 is frequently substituted by Lys in natural TEM variants having an extended profile for cephalosporins, but to date no substitutions for Asp104 have been found in SHV variants (*9*, *24*). We will discuss below how the Asp/Glu104 difference in SHV/TEM may contribute to their great differences in binding to BLIP.

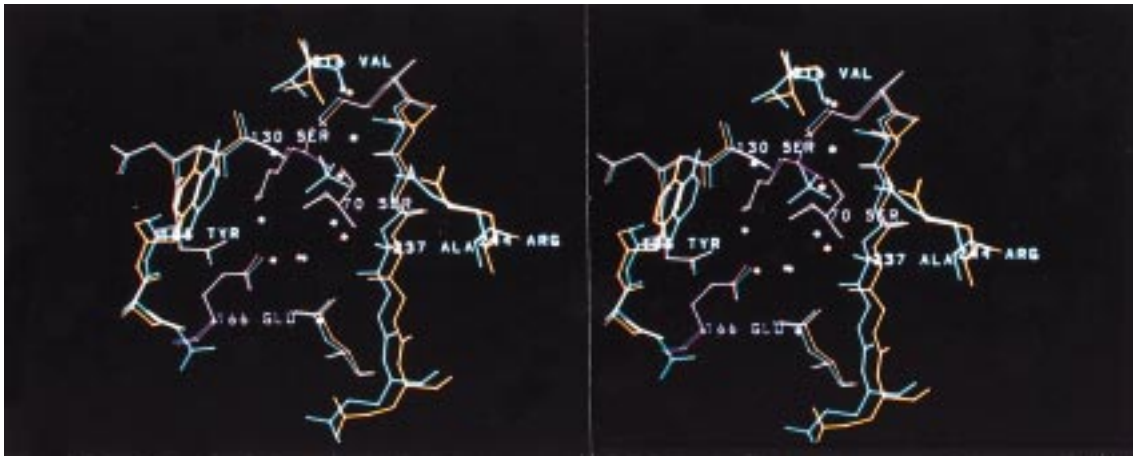

FIGURE 6: Overlay of active sites in the SHV-1 (yellow) and TEM-1 (1XPB, blue) β-lactamases. Water molecules are marked. Minimization was based on all atoms in residues 70, 73, 130, 132, 166, and 234. Orientation is similar to that in previous figures.

Table 3: Catalytic Site Distances (Å)

protein−protein		distance (av)[a]
Ser70OG	Lys73NZ	2.63 (2.70)
Ser130OG	Lys73NZ	3.59 (3.55)
Ser70OG	Ser130OG	3.31 (3.25)
Ser130OG	Lys234NZ	2.72 (2.90)
Lys73NZ	Asn132OD1	3.10 (2.70)
Ser70N	Ala237N	4.94 (4.70)
Ser70OG	Lys234NZ	4.52 (4.55)
protein−water		**distance**
Ser70OG	W317	2.92
Glu166OE2	W317	2.42
Asn170OD1	W317	3.02
Ser70N	W310	3.32
Ala237N	W310	2.73
Asn132OD1	W384	3.17
Asn132ND2	W384	3.34
Asp214OD1	W305	3.06
Lys234NZ	W305	3.04
Thr235OG1	W305	2.86
Thr235OG1	W386	3.90

[a] An average from four structures of three class A β-lactamases (*26*) is given in parentheses.

On the right side of the mouth along the β-strand, Gly238 is exclusively substituted by Ser in most SHV variants (8 of 12) and in at least 16 of the more than 60 TEM variants. Lower on the β-strand (and adjacent to 238 in the consensus numbering), the solvent-exposed Glu240 is often found changed to Lys (only) in both SHV and TEM families. Attempts have been made to understand these natural mutations using site-directed mutagenesis and structure-based modeling (*28*−*32*). Perhaps our finding of a widened mouth in SHV-1 helps explain the observation that analogous substitutions in the 238 region in TEM and SHV variants do not elicit the same phenotypic response (*33*).

The Ω *Loop*. The possible role of the Ω loop (160−181) in influencing substrate spectra of class A and class C β-lactamases (*34*, *35*) has recently been much better defined by a crystallographic study of an engineered class A mutant lacking the entire Ω loop (*36*). In the SHV/TEM pair a sequence difference in the Ω loop at position 167 (Pro in TEM-1 to Thr in SHV-1) adds a methyl group into the cavity. The Glu166−Thr167 peptide bond in SHV-1 is found in the cis conformation, as in all crystal structures of class A β-lactamases. Two hydrogen bonds between conserved residues Glu166 and Asn136 stabilize the non-proline cis peptide and help to configure the Ω loop so that Glu166 and Asn170 can activate the catalytic water molecule. Two nonconservative sequence differences in the Ω loop at 175 (Gly to Asn in SHV-1) and 177 (Ala to Glu) produce solvated side chains and do not result in differences in backbone conformation. As mentioned earlier, a possibly significant difference is that one edge of the Ω loop in SHV-1 (172−176) appears to have additional stabilization, not present in the TEM-1 enzyme, resulting from linkages with hydrogen-bonding residues Arg266 and Asp267 on the β-sheet.

At Asp179 a salt bridge is made to Arg164 across the neck of the Ω loop, a feature conserved in class A β-lactamases. Natural substitutions appear in these two residues in the SHV and TEM families, but only singly in each family. Variants at position 179 are found in SHV variants, while variants at position 164 are found in TEM variants. We observe that the environments and conformational angles of these two residues in the parental SHV-1 and TEM-1 structures are equivalent, showing that the cause for this two-path variation is not a local difference in structure.

Water Molecules. The catalytic site of SHV-1 contains five ordered water molecules. As in all class A β-lactamases, one of these waters (here W310) is in the oxyanion hole with hydrogen bonds to the backbone amide groups of Ser70 and Ala237 (Table 3), and it would be displaced by a substrate's β-lactam carbonyl group. The catalytically primed water molecule (W317) is strongly hydrogen bonded to Glu166 in the Ω loop, with additional hydrogen bonds to Asn170 and Ser70. A well-ordered water molecule (W305) lies between Asp214, Lys234, and Thr235. In the superposed SHV-1 and TEM-1 crystal structures (Figure 6), these three water molecules lie within 0.4−1.0 Å of one another.

The remaining two molecules in SHV-1 are in positions variable from one β-lactamase structure to another. One (W384) is weakly bonded to Asn132, and the other (W386) near Thr235 is clearly ellipsoidal in shape and may in fact be two disordered water molecules. In other structures this site is often occupied by tetrahedral anions such as sulfate (*12*, *13*) and cacodylate (*21*) or by an unknown species (*37*). Among these five water molecules in SHV-1, there are no inter-water distances less than 3.3 Å.

Table 4: Inhibition Constants (K_i, nM) for BLIP and β-Lactamases

β-lactamase	K_i	ref
SHV-1	1000	*25*
TEM-1	0.11, 0.3−0.4, 0.6	*25*, *38*, *39*
TEM-1 (E104K)	140	*25*
TEM-1 (G238S)	0.07	*25*
TEM-3	0.3	*38*

The water molecule normally seen bridging between the guanidinium group of Arg244 and the carbonyl group of Val216 (Figure 6) is not seen here, likely a result of Cymal-6 binding near 222−226 on H10. The backbone ϕ/ψ angles of Val216 are altered from −115°/10° in TEM-1 to −75°/−52° in SHV-1. This conformation rotates the 216 carbonyl group slightly away from Arg244, possibly releasing the bridging water molecule. This water molecule has been implicated in the mechanism of clavulanate inhibition of class A β-lactamases (*44*), and its loss may explain our difficulty in detecting a clavulanate intermediate by cryocrystallography (unpublished data).

Several other water molecules stabilize folding. These structural water molecules have low *B*-factors and bind not to mutatable side chains but to peptide backbone groups. Of the 63 water hydrogen bonds to peptide groups, twice as many (43) involve carbonyl groups than amide groups (20). Many internal hydration interactions are conserved in all class A β-lactamases (*21*). An example is the N-cap water molecule W302 which helps position Ser70 relative to the Ω loop containing the catalytic site residues Glu166 and Asn170:

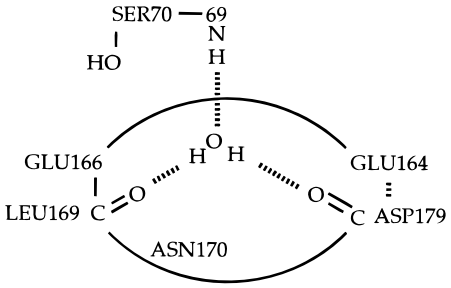

BLIP Binding. The 17.5 kDa β-lactamase inhibitory protein of *Streptomyces clavuligerus* binds to the class A β-lactamases with a broad range of K_i (*25*, *38*, *39*). The crystal structure of the BLIP/TEM-1 complex has been reported (*40*). Factors in the inhibition are hydrogen binding between AspB49 of BLIP and four catalytic residues in the β-lactamase and binding by PheB142 of BLIP in the site normally occupied by the benzyl ring of penicillin-G. The intermolecular binding generally occurs along a large surface formed by β-lactamase residues 99−112.

BLIP binds SHV-1 much more weakly than TEM-1 (Table 4). Electrostatic factors (*39*) and differences in pK_I (7.6 for SHV vs 5.4 for TEM) may influence binding. To search for a structural basis for this difference in binding, a virtual BLIP/SHV-1 complex was constructed by overlaying the SHV-1 and BLIP/TEM-1 crystal structures, but minimizing only 115 residues nearest the BLIP interface. The α-carbon atoms of SHV-1 and TEM-1 fit within 0.65 Å rms. Simple to rationalize in the weakening of BLIP binding to SHV-1 is the sequence change at position 124 (Ser in TEM-1 to Ala in SHV-1), which removes a hydrogen-bonded water bridge to BLIP SerB35. This, however, is only one of the many interactions documented in BLIP/TEM-1 binding (*40*). Other notable side chain differences at the interface occur at positions 100 (Asn to Gln in SHV-1), 104 (Glu to Asp), and 215 (Lys to Arg). These differences are conservative in character, but they involve a change in side chain size. Electrostatic binding by Glu104 and Lys215 exists in the BLIP/TEM-1 complex. Of the two attractions, the Glu104 linkage is better structured and is nearer the catalytic site (Figure 7). Shortening Glu104 to aspartic acid in SHV-1 (and lengthening Lys215 to arginine) may necessitate a global shift or rotation of BLIP, moving PheB142 from the β-lactam site and producing multiple perturbations elsewhere along the interface.

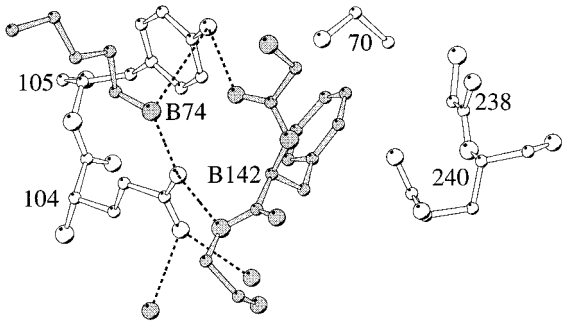

FIGURE 7: Binding of BLIP residues (LysB74 and PheB142) to the TEM-1 β-lactamase near Glu104 (*40*).

The published BLIP binding data for SHV-1, TEM-1, and TEM variants are rather dissimilar (Table 4). If we accept that the structural changes above could result in a 2000−9000-fold lower binding affinity for SHV-1, why does the engineered mutant of TEM-1, with a more radical change at 104 (Glu to Lys), show only a 1000-fold lower affinity? Also unaccountable is the datum indicating that the natural TEM-3 variant, with the same radical change at 104 (Glu to Lys), maintains strong BLIP binding! Does the additional change in TEM-3 at 238 (Gly to Ser) counter the change at 104? The datum for the Gly238 to Ser TEM-1 mutant does not support such a counter effect. It appears that more study is needed to resolve these binding data before structural conclusions can be drawn.

ACKNOWLEDGMENT

We thank L. B. Rice and V. Anderson (VA Medical Center) for technical assistance.

REFERENCES

1. Frere, J.-M. (1995) *Mol. Microbiol. 16*, 385−395.
2. Medeiros, A. A. (1997) *Clin. Infect. Dis. 24* (Suppl. 1), S19−S45.
3. Massova, I., and Mobashery, S. (1998) *Antimicrob. Agents Chemother. 42*, 1−17.
4. Joris, B., Ledent, P., Dideberg, O., Fonze, E., Lamotte-Brasseur, J., Kelly, J. A., Ghuysen, J.-M., and Frere, J.-M. (1991) *Antimicrob. Agents Chemother. 35*, 2294−2301.
5. Bush, K., Jacoby, G. A., and Medeiros, A. A. (1995) *Antimicrob. Agents Chemother. 39*, 1211−1233.
6. Jacoby, G. A., and Medeiros, A. A. (1991) *Antimicrob. Agents Chemother. 35*, 1697−1704.
7. Bonomo, R. A., Currie-McCumber, C., and Shlaes, D. M. (1992) *FEMS Microbiol. Lett. 92*, 79−82.
8. Zhou, X. Y., Bordon, F., Sirot, D., Kitzis, M.-D., and Gutmann, L. (1994) *Antimicrob. Agents Chemother. 38*, 1085−1089.

9. Bush, K., and Jacoby, G. (1997) *J. Antimicrob. Chemother. 39*, 1−3. For listing of all variants, see www.lahey.org/studies/webt.htm.
10. Knox, J. R., Zorsky, P. E., and Murthy, N. S. (1973) *J. Mol. Biol. 79*, 597−598.
11. Strynadka, N. C. J., Adachi, H., Jensen, S. E., Johns, K., Sielecki, A., Betzel, C., Sutoh, K., and James, M. N. G. (1992) *Nature 359*, 700−705.
12. Jelsch, C., Mourey, L., Masson, J.-M., and Samama, J.-P. (1993) *Proteins: Struct., Funct., Genet. 16*, 364−383.
13. Fonze, E., Charlier, P., Tóth, Y., Vermeire, M., Raquet, X., Dubus, A., and Frere, J.-M. (1995) *Acta Crystallogr. D51*, 682−694.
14. Johnson, B. H., and Hecht, M. H. (1994) *Biotechnology 12*, 1357−1360.
15. Lin, S., Thomas, M., Shlaes, D. M., Rudin, S. D., Knox, J. R., Anderson, V., and Bonomo, R. A. (1998) *Biochem. J. 333*, 395−400.
16. Navaza, J. (1994) *Acta Crystallogr. A50*, 157−163.
17. Sack, J. S. (1988) *J. Mol. Graphics 6*, 224−225.
18. Brunger, A. T. (1992) *X-PLOR: A system for X-ray crystallography and NMR, Version 3.1*, Yale University Press, New Haven, CT.
19. Brunger, A. T. (1992) *Nature 355*, 472−475.
20. Herzberg, O., and Moult, J. (1991) *Proteins: Struct., Funct., Genet. 11*, 223−229.
21. Knox, J. R., and Moews, P. C. (1991) *J. Mol. Biol. 220*, 435−455.
22. Lamotte-Brasseur, J., Dive, G., Dideberg, O., Charlier, P., Frere, J.-M., and Ghuysen, J.-M. (1991) *Biochem. J. 279*, 213−221.
23. Zafaralla, G., Manavathu, E. K., Lerner, S. A., and Mobashery, S. (1992) *Biochemistry 31*, 3847−3852.
24. Matagne, A., Lamotte-Brasseur, J., and Frere, J.-M. (1998) *Biochem. J. 330*, 581−598.
25. Petrosino, J., Rudgers, G., Gilbert, H., and Palzkill, T. (1999) *J. Biol. Chem. 274*, 2394−2400.
26. Knox, J. R., Moews, P. C., and Frere, J.-M. (1996) *Chem. Biol. 3*, 937−947.
27. Petit, A., Maveyraud, L., Lenfant, F., Samama, J.-P., Labia, R., and Masson, J.-M. (1995) *Biochem. J. 305*, 33−40.
28. Knox, J. R. (1995) *Antimicrob. Agents Chemother. 39*, 2593−2601.
29. Lee, K.-Y., Hopkins, J. D., O'Brien, T. F., and Syvanen, M. (1991) *Proteins: Struct., Funct., Genet. 11*, 45−51.
30. Huletsky, A., Knox, J. R., and Levesque, R. C. (1993) *J. Biol. Chem. 268*, 3690−3697.
31. Raquet, X., Lamotte-Brasseur, J., Fonze, E., Goussard, S., Courvalin, P., and Frere, J.-M. (1994) *J. Mol. Biol. 244*, 625−639.
32. Cantu, C., and Palzkill, T. (1998) *J. Biol. Chem. 273*, 26603−26609.
33. Venkatachalam, K. V., Huang, W., LaRocco, M., and Palzkill, T. (1994) *J. Biol. Chem. 269*, 23444−23450.
34. Herzberg, O., Kapadia, G., Blanco, B., Smith, T. S., and Coulson, A. (1991) *Biochemistry 30*, 9503−9508.
35. Lobkovsky, E., Moews, P. C., Liu, H., Zhao, H., Frere, J.-M., and Knox, J. R. (1993) *Proc. Natl. Acad. Sci. U.S.A. 90*, 11257−11261.
36. Banerjee, S., Pieper, U., Kapadia, G., Pannell, L. K., and Herzberg, O. (1998) *Biochemistry 37*, 3286−3296.
37. Herzberg, O. (1991) *J. Mol. Biol. 217*, 701−719.
38. Strynadka, N. C. J., Jensen, S. E., Johns, K., Blanchard, H., Page, M., Matagne, A., Frere, J.-M., and James, M. N. G. (1994) *Nature 368*, 657−660.
39. Albeck, S., and Schreiber, G. (1999) *Biochemistry 38*, 11−21.
40. Strynadka, N. C. J., Jensen, S. E., Alzari, P. M., and James, M. N. G. (1996) *Nat. Struct. Biol. 3*, 290−297.
41. Ambler, R. P., Frere, J.-M., Ghuysen, J.-M., Joris, B., Levesque, R. C., Tiraby, G., Waley, S. G., and Coulson, A. F. W. (1991) *Biochem. J. 276*, 269−272.
42. Jones, T. A. (1985) *Methods Enzymol. 115*, 157−170.
43. Kraulis, P. (1991) *J. Appl. Crystallogr. 24*, 946−950.
44. Imtiaz, U., Billings, E. M., Knox, J. R., Manavathu, E. K., Lerner, S. A., and Mobashery, S. (1993) *J. Am. Chem. Soc. 115*, 4435−4442.

BI990136D